Inorganica Chimica Acta 363 (2010) 2171–2179

Contents lists available at ScienceDirect

Inorganica Chimica Acta

journal homepage: www.elsevier.com/locate/ica

Synthesis, X-ray structures, electrochemical properties and cytotoxic effects of Co(II) complexes

Marta Sobiesiak [a], Krzysztof Sobiesiak [a], Agnieszka Mrozek [b], Peter Mayer [c], Ingo-Peter Lorenz [c], Marek Rozalski [d], Urszula Krajewska [d], Elzbieta Budzisz [a,e,*]

[a] Collegium Medicum in Bydgoszcz, Nicholaus Copernicus University in Torun, Faculty of Pharmacy, Department of Inorganic and Analytical Chemistry, 85-094 Bydgoszcz, Poland
[b] Institute of General and Ecological Chemistry, Technical University of Lodz, 90-924 Łódź, Poland
[c] Department of Chemistry and Biochemistry, Ludwig Maximilians University, Butenandtstr. 5-13 (D), D-81377 Munich, Germany
[d] Department of Pharmaceutical Biochemistry, Faculty of Pharmacy, Medical University of Lodz, Muszynskiego 1, 90-151 Lodz, Poland
[e] Medical University of Lodz, Faculty of Pharmacy, Department of Cosmetic Raw Materials Chemistry, 90-151 Lodz, Poland

ARTICLE INFO

Article history:
Received 23 October 2009
Received in revised form 22 February 2010
Accepted 3 March 2010
Available online 12 March 2010

Keywords:
Synthesis of cobalt(II) complexes
Cyclic voltammetry
Cytotoxicity
X-ray structures

ABSTRACT

1-Benzothiazol-2-yl-3,5-dimethyl-1*H*-pyrazole (**1a**) and 1-benzothiazol-2-yl-5-(2-hydroxyphenyl)-3-methyl-1*H*-pyrazole-4-carboxylic acid methyl ester (**1b**) were reacted with the hexahydrates of cobalt(II) chloride, cobalt(II) nitrate and cobalt(II) perchlorate to give the corresponding complexes **2a**–**4a** and **2b**–**5b**, respectively. Obtained compounds differ in coordination spheres of central atoms. The complex **2a** includes a fivefold coordinated cobalt(II) ion, whereas **3a** shows a distorted octahedral configuration around the cobalt(II) ion. All complexes were characterised by FTIR spectroscopy, MS and elemental analysis. The X-ray structures of **2a**, **3a** and **5b** complexes were also solved. The cytotoxic properties of the ligand **1a** and both series of Co(II) complexes were examined on human leukemia NALM-6 and HL-60 cells and melanoma WM-115 cells. The ligands, were found to have very low cytotoxicity. Complex **3b** exhibited the highest cytotoxic activity with IC_{50} values in the range of 6.9–17.1 μM for three examined cell lines.

1. Introduction

For many years we have been investigating the synthesis and cytotoxic activity of metalions-complexes with pyrazoles [1–4]. These five-membered heterocyclic compounds possess promising pharmacological, agrochemical and analytical applications [5]. The pyrazole-containing derivatives have been used as ligands in the formation of transition-metal complexes. The antitumor activity of these complexes is comparable with that of cisplatin [6–9].

The increased interest in ligands containing nitrogen and/or sulfur and their Co(II) complexes is raised by the potential biological activity of these compounds. Many reports described activity of cobalt(II) complexes in many classes of nitrogen donors [10–12]. The complexes of imidiazoles, benzimidazoles-derivatives and related ligands with cobalt(II) have been used as effective antibacterial agents [13]. The thiosemicarbazones complexes of cobalt(II) showed moderate antibacterial activity against bacteria such as *Escherichia coli* and *Salmonella typhi* and have been examined for antifungal activity against *Aspergillus niger* and *Candida albicans* [14]. Co(II) with Schiff bases containing the –N=C–C=N– moiety derived from 4-amino-5-sulfanyl-1,2,4-triazoles exhibit antibacterial and antifungal properties [15]. Co(II) with pyrazole derivatives showed activity against the fungi *Alternaria alternata* and *Macrophomina phaseoli* [16]. There are also examples of cobalt(II) Schiff-based complexes with antitumour [17] and catalytic oxidation activity [18,19].

Cobalt(III) compounds have also been investigated for their biological activity and examined especially as tumour-selective cytotoxic agents because of their redox properties [20–23]. Nitrogen-based complexes of cobalt(III) with nitrogen mustards or Schiff bases have been investigated as promising antitumour agents namely, hypoxia-activated prodrugs [24–32].

This paper is a part of our research project of systematically investigating metal(II) ions-complexes with *N*,*N*- or *N*,*S*-ligands. Here we present the synthesis, X-ray structures of Co(II) complexes, electrochemical properties and cytotoxic data of the free ligands and their complexes.

* Corresponding author at: Collegium Medicum in Bydgoszcz, Nicholaus Copernicus University in Torun, Faculty of Pharmacy, Department of Inorganic and Analytical Chemistry, 85-094 Bydgoszcz, Poland.
E-mail address: elzbieta.budzisz@umed.lodz.pl (E. Budzisz).

0020-1693/$ - see front matter © 2010 Elsevier B.V. All rights reserved.
doi:10.1016/j.ica.2010.03.011

2. Experimental

2.1. Materials

All substances were used without further purification. The hexahydrates of cobalt(II) chloride, cobalt(II) perchlorate and cobalt(II) nitrate were purchased from Aldrich. $CDCl_3$ and DMSO-d_6 solvents for NMR spectroscopy were obtained from Dr. Glaser AG, Basel. Solvents for synthesis (acetonitrile, dichloromethane, diethyl ether, ethanol, ethyl acetate, methanol) were reagent grade or better and were dried according to standard protocols [33]. The melting points were determined using a Buechi Melting-Point B-540 apparatus and they are uncorrected. The IR spectra were recorded on a FTIR-8400S Shimadzu Spectrophotometer in KBr. For the new compounds, satisfactory elemental analyses were obtained using a PerkinElmer PE 2400 CHNS analyser. The conductance of the metal complexes was determined in DMSO on an Elmetron CPC-501 conductometer. The Shimadzu UV-2501 PC (UV–Vis) study was carried out to verify the stability of complexes in 10^{-3} M DMSO in 0.01 M phosphate buffer (pH 7.0) containing 0.9% NaCl (PBS) solution. The MS-FAB data were determined on Finnigan MAT 95 mass spectrometer (NBA, Cs^+ gun operating at 13 keV). The ligands: 1-benzothiazol-2-yl-3,5-dimethyl-1*H*-pyrazole [34] (**1a**) and 1-benzothiazol-2-yl-5-(2-hydroxyphenyl)-3-methyl-1*H*-pyrazole-4-carboxylic acid methyl ester [35] (**1b**) were prepared according to published methods.

2.2. Synthesis of the complexes

Caution! *Perchlorate salts are potentially explosive and were handled only in small quantities with care.*

2.2.1. Synthesis of bis{(μ_2-chlorido) (1-benzothiazol-2-yl-3,5-dimethyl-1H-pyrazole-N2,N3′)-dichlorido-cobalt(II)} ($Co_2(\mu\text{-}Cl)_2$ (**1a**)$_2Cl_2$) (**2a**)

Cobalt(II) chloride $CoCl_2{\cdot}6H_2O$ (59.5 mg, 0.25 mmol) was dissolved in 2 ml methanol and was added dropwise at room temperature to a stirred solution of ligand 1-benzothiazol-2-yl-3,5-dimethyl-1*H*-pyrazole (**1a** 57.3 mg, 0.25 mmol) in ethyl acetate (10 ml). The stirring was continued for another hour at room temperature and the reaction mixture was left standing overnight. A blue micro-crystalline product was obtained, filtered off and dried. Blue crystals of **2a** were obtained after a few days by recrystallising the precipitated product from acetonitrile solution by slow evaporation to diethyl ether. Yield: 54.8 mg (65%), m.p.: 303.5–305.1 °C. FTIR (KBr cm^{-1}): ν(C–CH_3) 2915; ν(C=N) 1574, 1521. MS-FAB (*m*/*z*): 288 (15%) [Co(**1a**)H]$^+$, 230 (100%) **1a**. *Anal.* Calc. for $C_{12}H_{11}N_3SCoCl_2$ (**2a**) (359.13 g/mol): C, 40.13; H, 3.09; N, 11.70. Found: C, 40.29; H, 3.21; N, 11.56%.

2.2.2. Synthesis of 1-benzothiazol-2-yl-5-(2-hydroxyphenyl)-3-methyl-4-methoxycarbonyl-1H-pyrazole-N2,N3′-dichlorido-cobalt(II) (Co(**1b**)Cl_2) (**2b**)

Cobalt(II) chloride $CoCl_2{\cdot}6H_2O$ (48.4 mg, 0.2 mmol) was dissolved in 1 ml methanol and was added dropwise at room temperature to a stirred solution of ligand 1-benzothiazol-2-yl-5-(2-hydroxyphenyl)-3-methyl-1*H*-pyrazole-4-carboxylic acid methyl ester (**1b** 73.6 mg, 0.2 mmol) in ethyl acetate (10 ml). The stirring was continued for another 3 h at room temperature and the reaction mixture was left standing overnight. Violet micro-crystalline product **2b** was obtained, filtered off and dried. Yield: 69.8 mg (72%), m.p.: 308.0–308.4 °C. FTIR (KBr cm^{-1}): ν(OH) 3278; ν(C–CH_3) 2953; ν(C=O) 1718, ν(C=N) 1612, 1519, ν(C–O–C) 1114, 1099. MS-FAB (*m*/*z*): 458.9 (46%) [Co(**1b**)Cl]$^+$, 423 (18%) [Co(**1b**)]$^{2+}$, 366 (24%) **1b**. *Anal.* Calc. for $C_{19}H_{15}N_3O_3SCoCl_2$ (**2b**) (495.19 g/mol): C, 46.07; H, 3.05; N, 8.48. Found: C, 45.95; H, 2.68; N, 8.35%.

2.2.3. Synthesis of aqua-(1-benzothiazol-2-yl-3,5-dimethyl-1H-pyrazole-N2,N3′)-(nitrato-O,O′)-nitrato-O-cobalt(II) (Co(**1a**)$(NO_3)_2{\cdot}H_2O$) (**3a**)

Cobalt(II) nitrate $Co(NO_3)_2{\cdot}6H_2O$ (43.7 mg, 0.15 mmol) was dissolved in 2 ml methanol and was added dropwise at room temperature to a stirred solution of ligand **1a** (34.4 mg, 0.15 mmol) in CH_2Cl_2 (10 ml). The reaction solution was stirred and refluxed for 72 h and then filtered. The filtrate was kept at room temperature by slow evaporation to diethyl ether, and after 3 weeks, red crystals of **3a** were obtained. Yield: 27.1 mg (42%), m.p.: 233.0–234.2 °C. FTIR (KBr cm^{-1}): ν(O–H) 3334; ν(C–CH_3) 2928; ν(C=N) 1577, 1520; ν(NO_3^-) 1383, 812. MS-FAB (*m*/*z*): 415 (4%) Co(**1a**)$(NO_3)_2$, 305 (10%) [Co(**1a**)(H_2O)]$^{2+}$, 230 (100%) **1a**. *Anal.* Calc. for $C_{12}H_{11}N_5SCoO_6{\cdot}H_2O$ (**3a**) (430.26 g/mol): C, 33.50; H, 3.04; N, 16.28. Found: C, 33.39; H, 3.18; N, 16.49%.

2.2.4. Synthesis of 1-benzothiazol-2-yl-5-(2-hydroxyphenyl)-3-methyl-4-methoxycarbonyl-1-H-pyrazole-N2,N3′)-dinitrato-O,O′-cobalt(II) (Co(**1b**)$(NO_3)_2$) (**3b**)

Cobalt(II) nitrate $Co(NO_3)_2{\cdot}6H_2O$ (30.0 mg, 0.1 mmol) was added at room temperature to a stirred solution of ligand **1b** (37.9 mg, 0.1 mmol) in CH_2Cl_2 (10 ml) **1b**. The reaction solution was stirred for 24 h and was kept at room temperature by slow evaporation to diethyl ether, and after 2 weeks, pink crystals of **3b** were obtained. Yield: 23.0 mg (51%), m.p.: 250 °C dec. FTIR (KBr cm^{-1}): ν(O–H) 3424; ν(C–CH_3) 2977; ν(C=N) 1563, 1515; ν(NO_3) 1382, 831. MS-FAB (*m*/*z*): 486 (7%) [Co(**1b**)NO_3]$^+$, 424 (35%) [Co(**1b**)]$^{2+}$, 366 (100%) **1b**. *Anal.* Calc. for $C_{19}H_{15}N_3O_3SCo(NO_3)_2{\cdot}H_2O$ (**3b**) (548.29 g/mol): C, 42.43; H, 3.61. Found: C, 41.62; H, 3.18%.

2.2.5. Synthesis of [bis(1-benzothiazol-2-yl-3,5-dimethyl-1H-pyrazole-N2,N3′)-cobalt(II)] diperchlorate (Co(**1a**)$_2(ClO_4)_2$) (**4a**)

Cobalt perchlorate $Co(ClO_4)_2{\cdot}6H_2O$ (73.2 mg, 0.2 mmol) was dissolved in 1 ml methanol and was added dropwise at room temperature to a stirred solution of ligand **1a** (91.7 mg, 0.4 mmol) in ethyl acetate (20 ml). The reaction solution was stirred for 5 h and then was kept at room temperature by slow evaporation to diethyl ether, and after one week, pink crystals of **4a** were obtained. Yield: 119 mg (82%), m.p.: 314.1–314.4 °C. FTIR (KBr cm^{-1}): ν(O–H) 3442; ν(C–CH_3) 3099; ν(C=N) 1580, 1517; ν(ClO_4^-) 1127, 616. MS-FAB (*m*/*z*): 618 (4%) [Co(**1a**)$_2$]$^{2+}ClO_4^-$, 517 (4%) [Co(**1a**)$_2$]$^{2+}$, 288 (8%) [Co(**1a**)]$^{2+}$, 230 (38%) **1a.** *Anal.* Calc. for $C_{24}H_{22}N_6S_2Co(ClO_4)_2{\cdot}1/2H_2O$ (**4a**) (725.44 g/mol): C, 40.23; H, 3.09; N, 11.73. Found: C, 39.73; H, 3.19; N, 11.58%.

2.2.6. Synthesis of [bis(1-benzothiazol-2-yl-5-(2-hydroxyphenyl)-3-methyl-4-methoxycarbonyl-1H-pyrazole-N2,N3′)-cobalt(II)] diperchlorate (Co(**2b**)$_2(ClO_4)_2{\cdot}2H_2O$) (**4b**)

Cobalt perchlorate $Co(ClO_4)_2{\cdot}6H_2O$ (20.2 mg, 0.055 mmol) was dissolved in 1 ml methanol and was added at room temperature to a stirred solution of ligand **1b** (40.1 mg, 0.11 mmol) in ethyl acetate (10 ml). The reaction solution was stirred and refluxed for 24 h and then was kept at room temperature by slow evaporation to diethyl ether, and after one week, brown-orange crystals of **4b** were obtained. Yield: 50.1 mg (92%), m.p.: 254–255.5 °C. FTIR (KBr cm^{-1}): ν(O–H) 3401; ν(C=O) 1710; ν(C=N) 1612, 1514; ν(C=C) 1569; ν(ClO_4^-) 1116, 265. MS-FAB (*m*/*z*): 793.4 (35%) [Co(**1b**)$_2$]$^{2+}$, 524 (3%) [Co(**1b**)ClO_4], 428 (100%) [Co(**1b**)]$^{2+}$, 366 (25%) **1b**. *Anal.* Calc. for $C_{38}H_{30}N_6O_6S_2Co(ClO_4)_2{\cdot}2H_2O$ (**4b**) (1024.56 g/mol): C, 44.23; H, 4.0. Found: C, 44.55; H, 3.64%.

*2.2.7. Synthesis of acetonitrile-(1-benzothiazol-2-yl-5-(2-hydroxyphenyl)-3-methyl-4-methoxycarbonyl-1H-pyrazole-N2,N3′)-dichlorido-cobalt(II) (Co(**2b**)Cl_2CH_3CN) (**5b**)*

Green crystals of **5b** were obtained after a few days by re-crystallizing 25 mg of the precipitated product **2b** from the acetonitrile solution by slow evaporation to diethyl ether. Yield: 13.5 mg (54%), m.p.: 320.5–321.0 °C. FTIR (KBr cm^{-1}): ν(OH) 3423, ν(C–CH_3) 2950; ν(C=O) 1720, ν(C=N) 1615, 1520; ν(C–O–C) 1113, 1098. MS-FAB (*m*/*z*): 534 (M, 7%), 459 (57%) [Co(**1b**)Cl]$^+$, 424 (22%) [Co(**1b**)]$^{2+}$, 366 (21%) **1b**. *Anal.* Calc. for $C_{19}H_{15}N_3O_3SCoCl_2{\cdot}CH_3CN$ (**5b**) (536.24 g/mol): C, 47.76; H, 3.49. Found: C, 47.04; H, 3.38%.

2.3. X-ray structure determinations of **2a**, **3a** and **5a**

All measurements of the crystal **2a** were performed on Kuma 4-CCD *k*-axis diffractometer with graphite-monochromated Mo Kα radiation at room temperature. The crystals were positioned at 62 mm from the KM4-CCD camera, 496 frames were measured at 1.5 intervals with a counting time of 25 s. The data were corrected for Lorentz and polarisation effects. Multi-scan absorption correction was applied. Data reduction and analysis were carried out with the Kuma Diffraction programs [UNIL IC & KUMA (2000), CrysAlis CCD, ver. 1.163; Kuma Diffraction Instruments GmbH, Wrocław, Poland]. The structures were solved by direct methods [36] and refined using SHELXL 93 [37]. The full-matrix least-squares refinement was based on F^2 and applied anisotropic temperature factors for all non-H atoms; positions of all H atoms were found from electron-density maps and were refined in riding model with the isotropic displacement parameters of 1.5 times the respective U_{eq} values for the parent atoms. Atomic scattering factors were obtained from SHELXL. X-ray data for **3a** and **5b** were collected at 200 K with Mo Kα radiation (λ = 0.71073 Å) with a Nonius KappaCCD diffractometer equipped with a rotating anode generator. The structure was solved by direct methods with SIR97 [38] and refined with SHELXL-97 by full-matrix least-squares on F^2 [39].

2.4. Redox properties

The electrochemical properties of these complexes have been studied by cyclic voltammetry in DMF solution. Voltammetric measurements were made with the aid of a PGSTAT12 AUTOLAB electrochemical analyser. Three electrodes were utilised in this system, a glassy carbon working electrode (GCE), a platinum-wire auxiliary electrode and silver wire in contact with 0.1 M $AgNO_3$ in an ACN reference electrode. The GCE with 3.0 mm diameter was manually cleaned with 1 μm alumina polish prior to each scan. All solutions were deaerated for 10 min, prior to measurements with pure argon. A blanket atmosphere of argon was maintained over the solution during measurements. The potentials were measured in 0.2 M [nBu$_4$N][BF_4]/DMF as the supporting electrolyte, using the [Fe(η^5-(C_5H_5)$_2$] in DMF ($E_{1/2}$ = +0.72 V) as the internal standard.

2.5. Biological assays

2.5.1. Cell cultures

Human skin melanoma WM-115 cells as well as human leukemia promyelocytic HL-60 and lymphoblastic NALM-6 cells were used. Leukemia cells were cultured in RPMI 1640 medium (Invitrogen, UK) supplemented with 10% fetal bovine serum and antibiotics (100 μg/ml streptomycin and 100 U/ml penicillin). For melanoma WM-115 cells, Dulbecco's minimal-essential medium (DMEM) was used instead of RPMI 1640. Cells were grown in 37 °C in a humidified atmosphere of 5% CO_2 in air.

2.5.2. Cytotoxicity assay by MTT

The cytotoxicity of ligand **1a**, the complexes **2a**–**4a**, as well as **2b**–**4b** carboplatin and cisplatin were determined by the MTT [3-(4,5-dimethylthiazol-2-yl)-2,5-diphenyltetrazolium bromide, Sigma, USA] assay as described [40]. Stock solutions of the analysed compounds were freshly prepared in DMSO and diluted with complete culture medium to obtain a concentration range from 10^{-7} to 10^{-3} M. Cells were exposed to the test compounds for 46 h, then MTT reagent was added and incubation was continued for 2 h. After incubation, MTT-formazan crystals were dissolved in 20% SDS and 50% DMF at pH 4.7 and absorbance was read at 562 nm on an ELISA-plate reader (ELX 800, Bio-Tek, USA). The values of IC_{50} (the concentration of test compound required to reduce the cells' survival fraction to 50% of the control) were calculated from concentration–response curves and used as a measure of cellular sensitivity to a given treatment. As a control, cultured cells were grown in the absence of drugs. Data points represent means from 2 to 4 experiments, each performed at 5 repeats ± S.D.

3. Results and discussion

3.1. Chemistry

Looking for effective antitumour agents, we have decided to synthesise Co(II) complexes. In our previous studies similar compounds were shown to possess chelating properties towards many ions [41,42].

For our project we chose the two similar ligands presented in Fig. 1. We were interested in how the ligands' structure influences the cytotoxic activity of the complexes. Six cobalt(II) complexes with 1-benzothiazol-2-yl-3,5-dimethyl-1*H*-pyrazole (**1a**) and 1-benzothiazol-2-yl-5-(2-hydroxyphenyl)-3-methyl-1*H*-pyrazole-4-carboxylic acid methyl ester (**1b**) as ligands were synthesised. Three Co(II) complexes with **1a** were obtained by alternatives to the Arali and Zhang method (see Scheme 1) [35,43]. Those authors have shown the synthesis and antibacterial studies of 1-benzothiazol-2-yl-3,5-dimethyl-1*H*-pyrazole complexes of cobalt(II), nickel(II) and copper(II). Unfortunately, the authors had not reported important data such as the reaction yield or melting points of compounds. We also would have been interested in the electrochemical properties, X-ray structure and cytotoxic activity of synthesised Co(II) complexes.

As a part of our systematic investigation we presented the synthesis of new chelating ligand 1-benzothiazol-2-yl-5-(2-hydroxyphenyl)-3-methyl-1*H*-pyrazole-4-carboxylic acid methyl ester (**1b**) and its complexes with platinum(II), palladium(II) and copper(II) ions. Cytotoxicity studies showed the high effectiveness of Cu(II) complexes for skin melanoma WM-115 cells. The Cu(II) and Pt(II) complexes were chosen for *BAX* and *P53* gene expression study [35].

The ligand **1b** in the reactions with cobalt(II) chloride, cobalt(II) nitrate and cobalt(II) perchlorate hexahydrate created the solid complexes **2b**–**5b** (Scheme 1). Two complexes (**2b**, **3b**) were formed in molar ratio 1:1 in ethyl acetate/methanol and

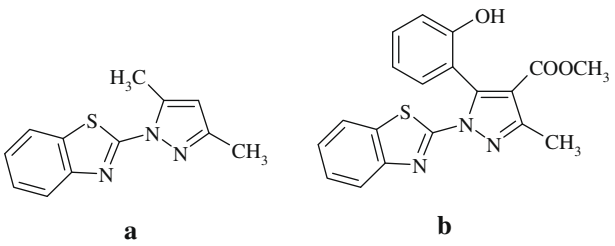

Fig. 1. The structure of ligands **1a** and **1b**.

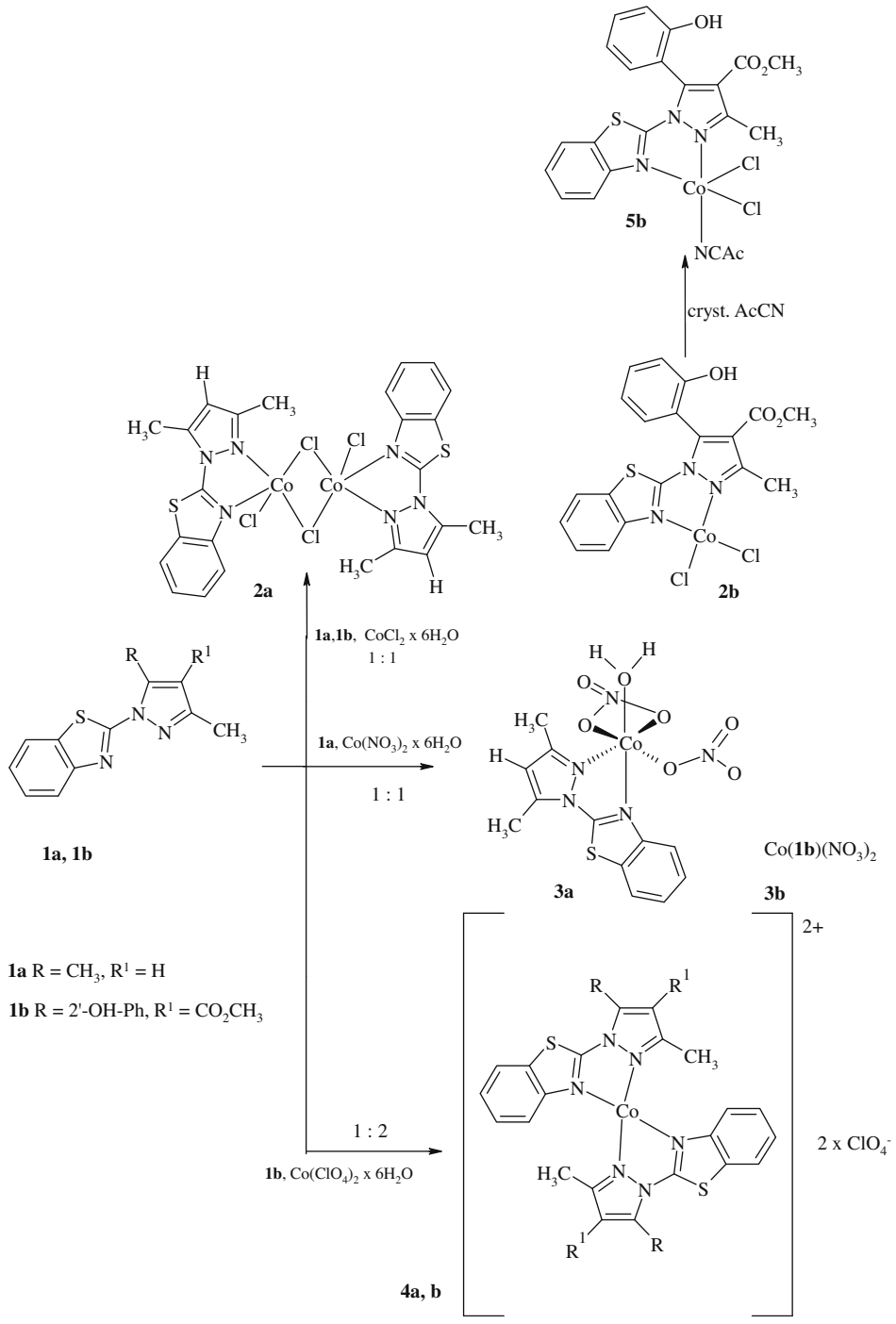

Scheme 1. Synthesis of Co(II) complexes **2a**, **2b**, **3a**, **3b**, **4a**, **4b** and **5b**.

dichloromethane solution, respectively. Ligand **1b** with cobalt(II) perchlorate hexahydrate in ethyl acetate solution formed the complex **4b** in molar ratio of 2:1. Single crystals of **3b** and **4b** have been obtained by slow diffusion of diethyl ether. Recrystallisation of the complex **2b** by the slow diffusion of diethyl ether into acetonitrile gave the cobalt(II) complex **5b**. We have been interested in electrochemical properties, X-ray structure and cytotoxic activity of synthesised new Co(II) complexes and which substituents in 4- or 5-position of the pyrazole ligands influence the cytotoxity of their Co(II) complexes.

The conductivity behaviour of complexes in DMSO was examined. The low conductivity values observed for complexes **2a**, **2b**, **3a**, **3b** in DMSO suggest that they are non-electrolyte but indicating solvation of the complexes. Complexes **4a** and **4b** are electrolytes in 10^{-3} M DMSO with values 97.4 and 95.0 ($ohm^{-1}\,cm^2\,mol^{-1}$), respectively. Therefore, the perchlorate anion is outside the metal coordination sphere.

The results of the UV–Vis study are shown in Table 1. Absorption spectra of DMSO/PBS solution complexes (10^{-6} do 10^{-4} M) were recorded in time intervals: $t = 0$ h, $t = 1$ h, $t = 2$ h, $t = 24$ h, $t = 48$ h. UV–Vis absorption spectra of ligands and their complexes showed characteristic peaks in the region of 250–350 nm. The absorption wavelength of complexes exhibited blue shifts compared with the ligands. The λ_{max} (nm) values of only two Co(II)

Table 1
UV–Vis data (λ_{max}) of compounds (**1a**,**b**–**4a**,**b**) in DMSO/PBS solution during 48 h.

Time (h)	0	1	2	24	48
Compound	λ_{max} (nm)				
1a	287	287	287	287	287
2a	289	290	288	288	290
3a	294	294	293	295	297
4a	296	296	296	296	296
1b	292	292	292	292	292
2b	297	297	297	297	297
3b	296	296	296	296	296
4b	295	295	295	295	295

compounds **2a**, **3a** were slightly changed during 48 h, meaning that the examined complexes were stable in solution.

3.1.1. MS-FAB

For valuable structural information Co(II) complexes **2a**,**b**–**4a**,**b** and **5b** were investigated by mass spectrometric measurement. Table 2 contains structurally informative molecular and fragment ions of cobalt(II) complexes. For all compounds in series **2a**–**4a** parent pick of complexes have not been observed in FAB-MS spectra. However, during the MS analysis the signals corresponding to their fragmentation ions CoL have been present. Moreover, for compound **2a** in FAB-MS spectra the following signals have been found: L_2Co_2Cl (M^+−683), $L_2Co_2Cl_2$ (M^+−647), CoLCl (M^+−323). This data are in good agreement with crystallographic study which suggests the dimeric structure for compound **2a**.

The FAB-MS analysis of compound **3a** has exhibited suitable fragmentation ion $CoLNO_3^+$ (M^+−350). For the compound **4a** two characteristic signals for this structure have been observed: CoL_2 (M^+−517) and CoL_2ClO_4 (M^++2H−618). The molecular ion peak of complex **5b** was found at (*m*/*z*) 534 indicating that complex corresponding to $CoLCl_2$ with one acetonitrile molecule. FAB-MS spectra of all complexes presented ion peak corresponded to ligand. For all complexes series **b** it was main fragment with *m*/*z* of 366 (100%). The molecular peaks for **3b** and 4**b** complexes corresponding to compounds with metal bonded to two ligand molecules at (*m*/*z*) 788 and 793. Additionally, a mass peaks of CoLCl (M^+−458), $CoLNO_3$ (M^+−486), $CoLClO_4$ (M^+−524), ions were observed in the mass spectra of coordination **2b**, **3b** and **4b**, respectively.

The presented above data are in good agreement with results obtained by elemental analysis, therefore confirm proposed by X-ray spectroscopy structure of investigated complexes.

3.1.2. IR analysis

The band in the 1512–1521 cm^{-1} region of the complexes **2a**, **2b**, **2a**, **3b**, **4a**, **4b**, **5b** has been assigned to C=N of the benzothiazole moiety. A shift of absorption bands characteristic to the vibrations of C=S group in region 580–700 cm^{-1} was absent in obtained spectra, indicating that the sulfur atom is not involved in coordination to cobalt(II). The infrared spectra showed that ligand–metal bonds in all obtained complexes were being created by nitrogen atoms and not by sulfur atoms. Comparative analysis of the infrared spectra of the complexes and the metal-free ligand has revealed that the absorption bands characteristic for the stretching vibrations of pyrazol C=N group were shifted from 1600 cm^{-1} for ligand **1a** to 1574, 1577, 1780 cm^{-1} for complexes **2a**, **3a**, and **4a** as a consequence of the *N* coordination. The intensive, broad band in the 3000–3600 cm^{-1} region is exhibited by a water molecule enclosed in **2a**. The band at 1715 cm^{-1} in the spectra of ligand **1b**, which has been assigned to the C=O vibrations, is now shifted to higher energies for the complexes **2b**, **3b**, **5b** (1722–1718 cm^{-1}). The IR-bands at 3416–3056 cm^{-1} in the spectra of the ligand **1b** and complexes **3b**–**5b** are assigned to the hydroxy group of the phenyl ring. The characteristic bands at 3103–2915 cm^{-1} of the methyl group of the ligand **2b** and its complexes **3b**–**5b** are assigned to C–H vibration. The presence of two bands between 1300–1400 cm^{-1} (very strong) and 800–860 cm^{-1} (medium) shows that **3a** and **3b** include NO_3^- ions. The bands observed at 1127, 617 and 1116, 626 cm^{-1} in the spectra of **4a** and **4b** are characteristic for non-coordinated perchlorate ions [44]. These observations correspond with crystallographic data obtained from X-ray structure analysis of these complexes.

Table 2
MS data (*m*/*z*) of complexes **2a**,**b**–**4a**,**b**, **5b**.

Compound	Molecular ions	Fragment ions
2a		230.1, 288.4, 683, 647
3a		230.1, 305.1, 415.3
4a		230.1, 288.2, 618.2, 517.5
2b		366.2, 423.4, 458.9,
3b		788.0, 486.1, 424.0, 366.0
4b		793.4, 524.1, 428.2, 366.1
5b	534	459.0, 424.2, 366.1

3.2. X-ray structure analysis

X-ray structure analyses of the complexes **2a**, **3a** and **5b** were conducted. All details of the X-ray-structure analysis are summarised in Table 3 and selected geometrical parameters are shown in Table 4.

3.2.1. Structural discussion of *2a*

As shown in the crystallographic structure of the complex in Fig. 2a two cobalt centres are linked via two chlorido bridges forming centrosymmetric dimeric units. The third chlorido ligand as well as the bidentate pyrazole **1a** completes the five-coordinated environment around the cobalt atom. The metal ion is in distorted *trigonal-bipyramidal* coordination. The axial bond angle N1–Co–Cl2A is 167.23(5)°, while the equatorial bond angles around the central Co atom are 118.28(3), 118.30(5), 121.75(5). The Co atom is 0.167 Å above the plane defined by N3, Cl1A and Cl2, towards the Cl2A atom. Hence, for a complete geometry description, the two Co–N and three Co–Cl distances are essential. The Co–N1 and Co–N3 distances of 2.1570(18) and 2.0834(17), respectively, are typical within pyrazine-like ligands. The Co–Cl distances are about 0.3 Å longer than Co–N ones. For 4 four structurally similar Co complexes found in the Cambridge Crystallographic Database (CSD, version 1.10 of Nov 2008) [45,46] the average value of Co–N distance is 2.064 Å, while the average Co–Cl distance equals 2.3872 Å.

The molecular packing is depicted in Fig. 2b. The aromatic moieties form a stack down the *c*-axis with a distance of about 3.657 Å. No hydrogen bonds were identified in the discussed structure.

3.2.2. Structural discussion of *3a*

Complex **3a** contains four different ligands around the distorted octahedral Co(II) centre; they are the *N*,*N*′-chelating diimine ligand **1a**, one *O*-monodentate and one *O*,*O*′-bidentate nitrato ligand and one aqua ligand (Fig. 3a). As in **2a**, the functionalised diimine ligand **1a** is again planar, the most deviation from planarity is given with the torsion angle N1–C1–N2–N3 = 3.7(3)° caused by its chelating function from different directions with different neighbours.

The bonds Co–N (Co–N1 2.1266(18), Co–N3 2.0969(18) Å) are also slightly different but within the range of those in **2a**. The four Co–O bonds differ more. Whereas Co–O4 (2.0591(17) Å) of the aqua ligand and Co–O7 (2.0766(17) Å) of the nitrato-*O* ligand are the shortest, both Co–O1 (2.2471(18) Å) and Co–O2

Table 3
Crystal data and details of the structure determinations of **2a**, **3a** and **5b**.

	2a	**3a**	**5b**[a]
Net formula	$C_{12}H_{11}N_3SCo$	$C_{12}H_{13}N_5O_7SCo$	$C_{22}H_{19.75}Cl_2CoN_{4.50}O_{3.13}S$
M_r/g (mol^{-1})	359.13	430.26	559.155
Crystal size (mm)	0.2 × 0.15 × 0.16	0.15 × 0.14 × 0.08	0.16 × 0.10 × 0.02
T (K)	296(2)	200(2)	200(2)
Diffractometer	Kuma 4-CCD	Kappa CCD	Kappa CCD
Crystal system	monoclinic	triclinic	monoclinic
Space group	$P21/n$	$P\bar{1}$	$C2/c$
a (Å)	8.2185(3)	8.6816(3)	31.5577(8)
b (Å)	15.7480(6)	8.7267(2)	9.6036(3)
c (Å)	10.9946(4)	12.2007(4)	21.6625(5)
α (°)	90	86.688(2)	90
β (°)	101.982(1)	69.4420(17)	131.8696(14)
γ (°)	90	70.1178(17)	90
V (Å^3)	1391.97(9)	811.90(4)	4888.9(2)
Z	4	2	8
Calculated density (g cm^{-3})	1.714	1.76	1.51938(6)
μ (mm^{-1})	1.753	1.235	1.04
Absorption correction	multi-scan	none	none
Reflections measured	22888	7025	17300
R_{int}	0.028	0.0297	0.0514
Mean $\sigma(I)/I$	0.0132	0.0464	0.0465
θ Range	2.29–25.00	3.58–27.48	3.36–26.04
Observed reflections	2175	2843	3715
x, y (weighting schemes)	0.0342, 0.6987	0.0260, 0.3865	0.0284, 3.4552
Hydrogen refinement	geom	mixed	mixed
Reflections in refinement	2449	3702	4808
Parameters	174	243	316
Restraints	0	2	0
$R(F_{obs})$	0.032	0.0342	0.0331
$R_w(F^2)$	0.0655	0.0778	0.0781
S	1.08	1.055	1.034
Shift/error$_{max}$	0	0.001	0.001
Maximum/minimum electron-density (e Å^{-3})	0.364/−0.187	0.354/−0.35	0.323/−0.342

[a] Per formula unit not coordinated: 0.125 H_2O and 0.5 CH_3CN.

Table 4
Selected geometrical parameters of complexes **2a**, **3a** and **5b**.

2a				**3a**				**5b**			
Bond lengths (Å)		Bond angles (°)		Bond lengths (Å)		Bond angles (°)		Bond lengths (Å)		Bond angles (°)	
Co–N1	2.1570(18)	Cl1–Co–Cl2	118.28(3)	Co–N1	2.1266(18)	N1–Co–N3	76.84(7)	Co–Cl1	2.3218(7)	Cl1–Co–Cl2	119.69(4)
Co–N3	2.0834(17)	N1–Co–N3	75.99(7)	Co–N3	2.0969(18)	O1–Co–O2	58.15(6)	Co–Cl2	2.2671(12)	Cl1–Co–N1	87.60(5)
Co–Cl1	2.2684(7)	Cl2A–Co–N1	167.23(5)	Co–O1	2.2471(18)	O1–Co–N3	91.55(6)	Co–N1	2.1507(18)	Cl1–Co–N3	120.81(7)
Co–Cl2	2.3581(7)	Cl2A–Co–N3	99.53(5)	Co–O2	2.1634(17)	O1–Co–N1	95.38(7)	Co–N3	2.123(2)	Cl1–Co–N	490.31(6)
Co–Cl2A*	2.4166(7)	N3–Co–Cl1	118.30(5)	Co–O4	2.0591(17)	O1–Co–O4	174.68(6)	Co–N4	2.102(2)	Cl2–Co–N1	94.70(7)
Co–CoA*	3.5190(8)	N1–Co–Cl1	94.25(5)	Co–O7	2.1266(18)	O2–Co–O4	117.67(7)	N4–C20	1.135(3)	Cl2–Co–N3	117.93(7)
		N3–Co–Cl2	121.75(5)	O1–N4	1.273(2)	O2–Co–O7	90.52(7)	C20–C21	1.449(4)	Cl2–Co–N4	96.79(8)
		N1–Co–Cl	287.27(5)	O2–N4	1.260(2)	O2–Co–N3	146.51(7)			N1–Co–N3	75.35(8)
		N3–Co–Cl2A*	99.53(5)	O3–N4	1.223(3)	N3–Co–O4	93.31(7)			N1–Co–N4	167.78(11)
		Cl1–Co–Cl2A*	98.37(2)	O4–N5	1.271(2)	N3–Co–O7	102.41(7)			N3–Co–N4	95.51(9)
		Cl2–Co–Cl2A*	85.03(2)	O5–N5	1.235(3)	N1–Co–O7	177.97(7)			Co–N4–C20	176.6(2)
				O6–N5	1.241(2)	N1–Co–O4	87.84(7)				
Torsion angles (°)											
N1–C7–N2–N3	4.1(4)			N1–C1–N2–N3	3.7(3)			N1–Co–N3–N2	−12.97(17)		
N1–Co–N3–N2	1.9(11)			N1–Co–N3–N2	1.8(13)			N1–C1–N2–N3	−13.4(3)		
Hydrogen bridges											
				O7–H71–O6[35] 0.844(10), 1.907(12), 2.739(2), 168(3)				O1···H1···Cl1i 0.78(3), 2.33(3), 3.102(2), 175(4)			
				O7–H72–O1[36] 0.827(10), 2.261(16), 3.020(2), 153(3)				(i = 1/2 − x, 1/2 + y, 1/2 − z)			

C-bonded H: constr; O-bonded H: O–H fixed to 0.84 Å, U(H) = 1.5 × U(O).
* Cl2A and CoA denotes the symmetry equivalents of atoms Cl2 and Co.

(2.1634(17) Å) of the nitrato O,O' ligand are significantly longer and, additionally, they are not equal. As expected, the nitrato ligands are planar and the N–O bond lengths lie in the range of 1.223(3) (N4–O3) to 1.271(2) Å (N5–O4) depending on whether coordinated or not. Of the two of the bite-angles, that of O1–Co–O2 = 58.15(6)° is much smaller than N1–Co–N3 (76.84(7)°) (**2a**: 75.97(6)°) because of its four-membered ring situation. The monodentate nitrato ligand is slightly bent off the molecular plane defined by O1, O2, O4 and N3 with the torsion angle Co–O4–N5–O5 = −8.5(2)° (Fig. 3b).

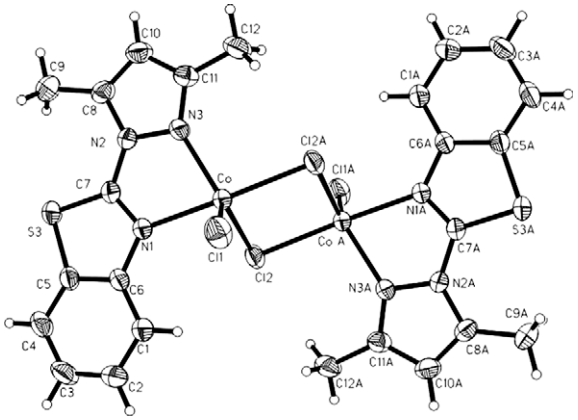

Fig. 2a. An ORTEP drawing of **2a** with atom numbering. The non-hydrogen atoms are shown with 50% probability ellipsoids.

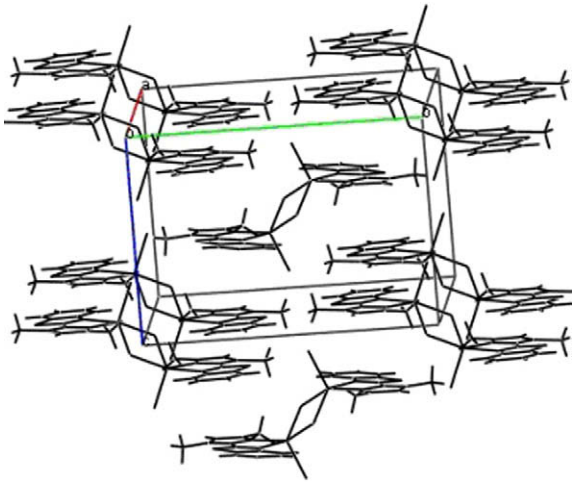

Fig. 2b. Stacking of **2a** molecules down the *c*-axis.

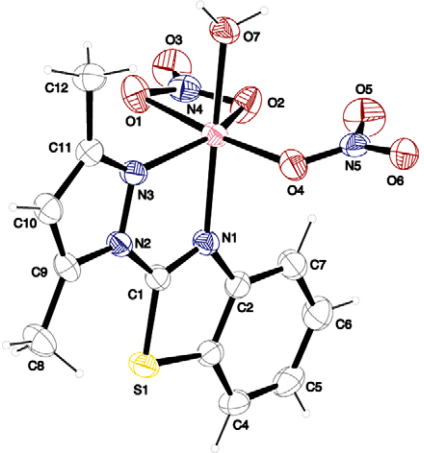

Fig. 3a. An ORTEP drawing of **3a** with atom numbering. The non-hydrogen atoms are shown with 50% probability ellipsoids.

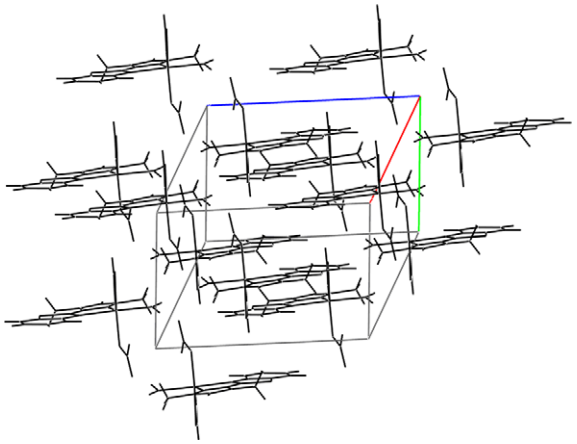

Fig. 3b. Stacking of **3a** molecules down the *c*-axis.

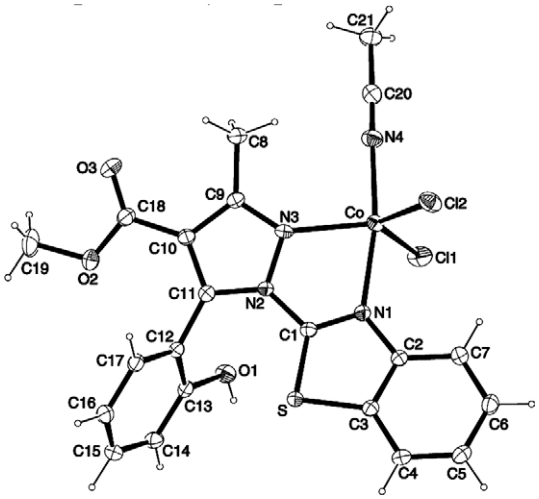

Fig. 4a. An ORTEP drawing of **5b** with atom numbering. The non-hydrogen atoms are shown with 50% probability ellipsoids.

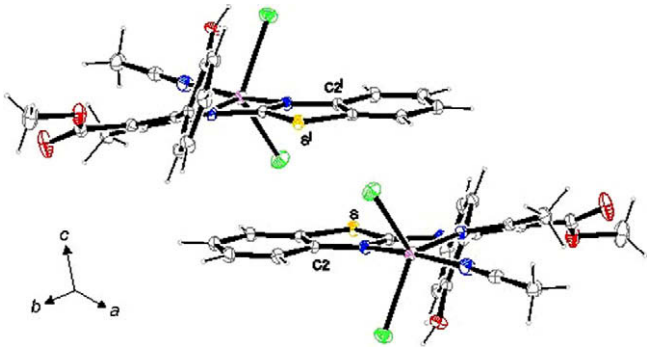

Fig. 4b. π–π-stacking in **5b** within the *c*-axis ($i = 0.5 - x, 0.5 - y, 1 - z$). The non-coordinating solvate molecules H_2O and CH_3CH are omitted.

3.2.3. Structural discussion of ***5b***

The Co(II) centre in complex **5b** shows a distorted trigonal-bipyramidal configuration with two chlorido ligands and atom N3 of the chelate system in equatorial positions (Cl1–Co–Cl2 119.69(4), Cl1–Co–N3 120.81(7), Cl2–Co–N3 117.93(7)°) (see Fig. 4a). The other chelating atom N1 and N4 of the coordinating CH_3CN lie in trans-axial positions (N1–Co–N4 167.78(11)°). The angles between equatorial and apical ligands vary from 87.60(5)° (Cl1–Co–N1) to 96.79(8)° (Cl2–Co–N4) with the only exception being angle N1–Co–N3 75.35(8)° due to its bite-angle character. The acetonitrile

ligand is nearly linearly bonded (Co–N4–C20 176.6(2)°). Although in apical position, it shows the shortest Co–N bond (Co–N4 2.102(2) Å); its counterpart, Co–N1 2.151(2) Å, however, the longest one (Co–N3 2.123(2) Å). Both bond lengths Co–Cl differ somewhat (Co–Cl1 2.3218(7), Co–Cl2 2.2672(2) Å), but they lie, as do the Co–N distances, in the range of **2a** and **3a**. With the torsion angles N1–C1–N2–N3 −13.4(3)° and N1–Co–N3–N2 −12.97(17)°, the ligand itself, as well as the five-membered metallacycle are again planar. In contrast to **3a** with two intramolecular O···H···O bridges, there is an intermolecular hydrogen bridge between the chlorido ligand Cl1 and the oxygen of the non-coordinate solvate molecule H_2O. Between the five-membered rings of the benzothiazole part of **5b** a π–π-stacking is observed with the shortest distances between S and C2[1] or C2 and S[i] (3.457(3) Å) (Fig. 4b).

3.3. Cyclic voltammetry

Electrochemical studies of cobalt(II) complexes have been done in connection with the investigation of their biological properties.

The cyclic voltammogram of complex **2a** shows two waves at −0.110 V and −1.380 V. The peak-to-peak separation (ΔE_p) amounts to 1.27 V and proportion of the anodic peak current (i_{pa}) and the cathodic peak current (i_{pc}) indicate a quasireversible process. A representative illustration is given in Fig. S5.

The voltammogram of complex **2b** shows two waves at 0.052 V and −0.827 V (Fig. S6). The peak-to-peak separation (ΔE_p) amounts to 0.879 V and proportion of the anodic peak current (i_{pa}) and the cathodic peak current (i_{pc}) indicate a quasireversible process. The reduction potential of **2b** is the highest of analysed complexes, therefore peak-to-peak separation value is lowest of them.

The cyclic voltammograms of **3a**, **3b**, **4a**, **4b** are similar (Figs. S7–S10). They show one reduction and one oxidation wave. Potentials of reduction waves are in the range from −1.238 V to −1.340 V. Potentials of oxidation waves are in the range from −0.091 V to 0.070 V. The peak-to-peak separation (ΔE_p) of higher than 1.180 V and proportion of the anodic peak current (i_{pa}) and the cathodic one (i_{pc}) indicates a quasireversible process. All these results are consistent with a quasireversible behaviour. These obtained voltammograms exhibit one step reduction process from $Co^{2+} \rightarrow Co^{1+}$ which is probably stabilized by the ligand environment. This fact explains the high value of peak-to-peak separation according to a quasireversible process.

Complex **2a** shows one additional reduction peak at −2.090 V like complex **2b** at −1.953 V. Both complexes include chlorido ligands in the structure. The cyclic voltammograms of both ligands **1a**, **1b** do not exhibit any waves. The oxidation and reduction potentials and peak-to-peak separation values of all investigated complexes are gathered in Table 5.

3.4. Biological assays

3.4.1. Cytotoxicity studies

The cytotoxicity of ligands **1a**, **1b** and their Co(II) complexes **2a**,**b**–**4a**,**b** was assayed against melanoma WM-115 cells as well as leukemia promyelocytic HL-60 and lymphoblastic NALM-6 cells. Cisplatin and carboplatin were used as the reference compounds. The cells were exposed to a broad range of drug concentrations (10^{-7} to 10^{-3} M) for 48 h and cell viability was analysed by MTT assay. IC_{50} values are presented in Table 6. Metal complexes **2a**–**4a** and **4b** exhibited rather moderate cytotoxicity to leukemia HL-60 cells although complex **2b** was more active. Relatively high cytotoxic activity with an IC_{50} of 6.9–9.7 μM was observed for complexes **2b**, **3a**, **3b**, **4a**, **4b** in the case of lymphoblastic NALM-6 cells. The complexes **3b** and **4b** exhibited higher cytotoxic activity in the case of skin melanoma WM-115 cells. The cytotoxic effectiveness of these compounds with an IC_{50} of 8.9 μM (**3b**) and 20.3 μM (**4b**) was higher or comparable to that of cisplatin (18.2 μM) and was much higher than that of carboplatin (422.2 μM). It should also be mentioned that ligands **1a** and **1b** presented low toxicity.

Table 5
Electrochemical oxidation potential (E_{pa}), reduction potentials (E_{pc}) and peak-to-peak separation (ΔE_p) of analysed complexes.

Compound	E_{pa1}	E_{pc1}	ΔE_{p1}	E_{pa2}	E_{pc2}	ΔE_{p2}
2a	−0.110	−1.380	1.270		−2.090[a]	
2b	0.052	−0.827	0.879		−1.953[a]	
3a	−0.058	−1.238	1.180			
3b	−0.091	−1.340	1.249			
4a	0.070	−1.240	1.240			
4b	−0.020	−1.330	1.310			

[a] Only irreversible reduction.

Table 6
Cytotoxic activity (μM)[a] of ligand **1a**, **1b** and their Co(II) complexes **2a**,**b**–**4a**,**b**, cisplatin and carboplatin to HL-60, NALM-6 and WM-115 cells.

Compound	Cytotoxicity (μM)[a]		
	HL-60	NALM-6	WM-115
1a	368.8 ± 18.8	367.4 ± 22.2	743.8 ± 76.4
1b[b]	>1000	74.0 ± 12.9	55.1 ± 8.2
2a	46.3 ± 3.8	44.4 ± 5.4	69.8 ± 2.3
2b	10.2 ± 1.7	7.5 ± 0.1	54.1 ± 7.7
3a	41.6 ± 4.6	9.7 ± 0.3	77.9 ± 8.9
3b	17.1 ± 3.0	6.9 ± 0.1	8.9 ± 0.3
4a	45.4 ± 6.4	7.1 ± 0.3	88.1 ± 3.1
4b	24.6 ± 4.0	8.0 ± 0.2	20.3 ± 3.1
Cisplatin	0.8 ± 0.1	0.7 ± 0.3	18.2 ± 4.3
Carboplatin	4.3 ± 1.3	0.7 ± 0.2	422.2 ± 50.2

[a] IC_{50}-concentration of a tested compound to reduce the fraction of surviving cells to 50% of that observed in the control, non-treated cells. Mean values of IC_{50} (in μM) ± S.D. from 2 to 4 experiments each performed in quintuple are presented.
[b] See literature [35].

4. Conclusions

We have investigated in this paper the synthesis, X-ray structures, electrochemical properties, and cytotoxic effect of cobalt(II) complexes. Their synthesis from the hexahydrates of $CoCl_2$, $Co(NO_3)_2$, and $Co(ClO_4)_2$ as substrates resulted in new and different structures. The electrochemical behaviour of analysed complexes shows a quasireversible (ΔE_p higher than 0.879 V) process.

Preliminary cytotoxic studies indicate that cobalt(II) complexes with ligand **1a** display acceptable, but less cytotoxic activity as compared to cisplatin and carboplatin. Cobalt(II) complexes with ligand **1b** were found to display higher cytotoxic activity as compared to **2a**–**4a** and even as compared to that of reference compounds. The complexes **3b** and **4b** exhibited higher cytotoxic activity in NALM-6 and WM-115 cell lines. Therefore, these complexes could serve as cobalt models for further cytotoxic studies. The free ligand **1a** presented low cytotoxicity in comparison to **1b**. Both examined ligands possess the pyrazole and benzothiazole moiety. The cytotoxity studies indicate that substituents in the 4- or 5-position of the pyrazole molecules have an effect on their activity.

In complexes discussed, the dihedral angles N3–N2–C1–N1 have been found close to 0°. Moreover, shortening of the N2–C1, C1–S1 bonds and elongation of C1–N1 bond were observed. Additionally, in the octahedral complex, one of the oxygen atoms of the NO_3 group has been involved in the creation of the hydrogen bond with the apical water molecule. The natural population analysis has shown the charge transfer from ligands to metal centre under the charge comparison between the free ligand and the discussed complexes. These differences of spatial geometry and charge

distribution, were probably forced by different types of Co(II) complex formations.

Acknowledgements

Financial support from Grant No. 503-3066-2 to Prof. Budzisz and No. 503-3015-2 to Prof. Mirowski at Medical University of Lodz and Grant No. 411 at Collegium Medicum in Bydgoszcz are gratefully acknowledged.

Appendix A. Supplementary material

CCDC 740287, 737530 and 766529 contains the supplementary crystallographic data for **2a**, **3a** and **5b**. These data can be obtained free of charge from The Cambridge Crystallographic Data Centre via http://www.ccdc.cam.ac.uk/data_request/cif. Supplementary data associated with this article can be found, in the online version, at doi:10.1016/j.ica.2010.03.011.

References

[1] E. Budzisz, M. Małecka, B. Nawrot, Tetrahedron 1749 (2004) 60.
[2] E. Budzisz, U. Krajewska, M. Różalski, A. Szuławska, M. Czyż, B. Nawrot, Eur. J. Pharmacol. 59 (2004) 502.
[3] E. Budzisz, M. Malecka, B. Keppler, V.B. Arion, G. Andrijewski, U. Krajewska, M. Różalski, Eur. J. Inorg. Chem. (2007) 3728.
[4] E. Budzisz, I.-P. Lorenz, P. Mayer, P. Paneth, A. Szatkowski, U. Krajewska, M. Rozalski, M. Miernicka, New J. Chem. 2238 (2008) 32.
[5] J. Elguero, in: A.R. Katrizky, C.W. Rees, E.F. Scriven (Eds.), Comprehensive Heterocyclic Chemistry II, vol. 3, Pergamon, Oxford, 1996.
[6] R. Ahmad, N. Ahmad, M. Zig-Ui-Hag, A. Wahid, J. Chem. Soc. Pakistan 33 (1996) 18.
[7] M.Z. Wisniewski, W.J. Surga, E.M. Opozda, Transition Met. Chem. 19 (1994) 353–354.
[8] T.A.K. Al-Allaf, L.J. Rashan, Boll. Chim. Farm. 140 (2001) 205–210.
[9] N.J. Wheate, C. Cullinane, L.K. Webster, J.G. Collins, Anticancer Drug Des. 16 (2001) 91–98.
[10] S.O. Podunavac-Kuzmanovic, Ljiljana S. Vojinović, APTEFF 34 (2003) 119.
[11] I. Yilmaz, A. Cukurovali, Transition Met. Chem. 399 (2003) 28.
[12] W. Zeng, J.-Z. Li, Y. Du, X.-Y. Wei, S.-Y. Qin, React. Kinet. Catal. Lett. 79 (2003) 111.
[13] S.O. Podunavac-Kuzmanovic, D.M. Cvetkovic, G.S. Cetkovic, APTEFF 35 (2004) 231.
[14] R.K. Agarwal, S. Prasad, Bioinorg. Chem. Appl. 271 (2005) 3.
[15] M.S. Yadawe, S.A. Patil, Transition Met. Chem. 5 (1997) 220.
[16] N. Singh, N.K. Sangwan, K.S. Dhindsa, Pest Manage. Sci. 56 (2000) 284.
[17] R. Gust, I. Ott, D. Posselt, K. Sommer, J. Med. Chem. 47 (2004) 5837.
[18] A. Pui, C. Policar, J.-P. Mahy, Inorg. Chim. Acta 360 (2007) 2139.
[19] D. Chen, A.E. Martell, Y. Sun, Inorg. Chem. 28 (1989) 2647.
[20] A. Mishra, N.K. Kaushik, A.K. Verma, R. Gupta, Eur. J. Med. Chem. 43 (2008) 2189.
[21] J.B. Delehanty, J.E. Bongard, Dz.C. Thach, D.A. Knight, T.E. Hickeya, E.L. Changa, Bioorg. Med. Chem. 830 (2008) 16.
[22] T. Takeuchi, A. Böttcher, C.M. Quezada, T.J. Meade, H.B. Gray, Bioorg. Med. Chem. 815 (1999) 7.
[23] M.D. Hall, T.W. Failes, N. Yamamoto, T.W. Hambley, Dalton Trans. (2007) 3983.
[24] B. Teicher, M. Abrams, K. Rosbe, T. Herman, Cancer Res. 6971 (1990) 50.
[25] D.C. Ware, B.D. Palmer, W.R. Wilson, W.A. Denny, J. Med. Chem. 1839 (1993) 36.
[26] D.C. Ware, H.R. Palmer, P.J. Brothers, C.E. Rickard, W.R. Wilson, W.A. Denny, J. Inorg. Biochem. 215 (1997) 68.
[27] D.C. Ware, P.J. Brothers, G.R. Clark, W.A. Denny, B.D. Palmer, W.R. Wilson, J. Chem. Soc., Dalton Trans. (2000) 925.
[28] P.R. Craig, P.J. Brothers, G.R. Clark, W.R. Wilson, W.A. Denny, D.C. Ware, Dalton Trans. (2004) 611.
[29] S.P. Osinsky, I.Ya. Levitin, A.L. Sigan, L.N. Bubnovskaya, I.I. Ganusevich, L. Campanella, P. Wardmand, Russ. Chem. Bull., Int. Ed. 2636 (2003) 52.
[30] S. Osinski, I. Levitin, L. Bubnovskaya, A. Sigan, I. Ganusevich, A. Kovelskaya, N. Valkovskaya, L. Campanella, P. Wardman, Exp. Oncol. 140 (2004) 26.
[31] W. Failes, C. Cullinane, C.I. Diakos, N. Yamamoto, J.G. Lyons, T.W. Hambley, Chem. Eur. J. 2974 (2007) 13.
[32] E. Reisner, V.B. Arion, B.K. Keppler, A.J.L. Pombeiro, Inorg. Chim. Acta 1569 (2008) 361.
[33] J.T. Wrobel, Preparatyka i elementy syntezy organicznej, PWN, Warszawa, 1983. p. 9.
[34] V.H. Arali, V.K. Revankar, V.B. Mahale, Transition Met. Chem. 158 (1993) 18.
[35] E. Budzisz, M. Miernicka, I.-P. Lorenz, P. Mayer, E. Balcerczak, U. Krajewska, M. Rozalski, Eur. J. Med. Chem. doi:10.1016/j.ejmech.2010.02.050.
[36] G.M. Sheldrick, SHELXTL PC^MT, Siemens Analytical X-Ray Instruments Inc., Madison, Wisconsin, USA, 1990.
[37] G.M Sheldrick, SHELXL-93.A FORTRAN-77 Program for the Refinement of Crystal Structures from Diffraction Data, University of Göttingen, Germany, 1993.
[38] Ch.A. McFerrin, R.P. Hammer, F.R. Fronczek, S.F. Watkins, Acta Crystallogr. E E62 (2006) o2518.
[39] G.M. Sheldrick, SHELXL-97, 97-2 version, University of Göttingen.
[40] E. Budzisz, U. Krajewska, M. Rozalski, Pol. J. Pharmacol. 56 (2004) 473.
[41] A. Kufelnicki, M. Wozniczka, L. Checinska, M. Miernicka, E. Budzisz, Polyhedron 2589 (2007) 26.
[42] M. Miernicka, A. Szulawska, M. Czyz, I.-P. Lorenz, P. Mayer, B. Karwowski, E. Budzisz, J. Inorg. Biochem. 157 (2008) 102.
[43] Z.-G. Zhang, Y.-Y. Sun, X.-M. Jing, Acta Crystallogr. E 1307 (2005) 61.
[44] B. Stuart, Infrared Spectroscopy – Fundamentals and Applications, Wiley, Chichester, UK, 2004. p. 45.
[45] F.H. Allen, Acta Crystallogr. B58 (2002) 380.
[46] A.G. Orpen, Acta Crystallogr. B58 (2002) 398.